



Seismic collapse assessment of low-rise controlled rocking masonry wall with and without confinement

Ahmed Yassin¹, Mohamed Ezzeldin², Lydell Wiebe³

¹ Ph.D. Candidate, Department of Civil Engineering, McMaster University - Hamilton, ON, Canada.

² Postdoctoral Fellow, Department of Civil Engineering, McMaster University - Hamilton, ON, Canada.

³ Associate Professor, Department of Civil Engineering, McMaster University - Hamilton, ON, Canada.

ABSTRACT

Unbonded post-tensioned controlled rocking masonry walls (PT-CRMWs) show promise as a seismic force resisting system for resilient cities. This is mainly because of their ability to self-centre after a seismic event with minimal residual deformations compared to conventional fixed reinforced masonry (RM) wall systems, allowing for much more rapid return to occupancy for facilities due to the low wall damage. This self-centering ability is achieved by using unbonded post-tensioned tendons that also prevent any tensile stresses from transmitting to the masonry wall through bond. Therefore, only a single horizontal base crack typically forms at the wall-foundation interface, due to wall uplift and rocking during a seismic event. However, the current North American building codes (i.e. NBC and ASCE-7) and standards (i.e. CSA S304 and TMS 402) have not provided design requirements for PT-CRMW systems due to the lack of research on their performance.

In this study, a nonlinear numerical model is developed, validated, and used to evaluate the seismic collapse risk of low-rise PT-CRMWs following the FEMA P695 methodology, assuming seismic performance factors equal to those currently assigned to special RM shear walls in ASCE-7. Three walls are analyzed, each with and without confinement, representing one-, two-, and four-storey low-rise buildings. The results show that PT-CRMWs exhibit an enhanced performance that is enough to meet the FEMA P695 acceptance criteria for the expected seismic collapse risk under the maximum considered earthquake (MCE).

Keywords: *Collapse Risk, Nonlinear Dynamic Analysis, Rocking Masonry, Self-Centering, Unbonded Post-Tensioning.*

INTRODUCTION

The promising results of the Precast Seismic Structural Systems (PRESSSS) program [1] attracted researchers towards controlled rocking wall systems with vertical unbonded post-tensioning (PT). The PRESSSS test results for a controlled rocking precast concrete wall demonstrated that damage was concentrated at the wall toes with a single crack at the wall-foundation rocking interface and a permanent drift of only 0.06%, after a maximum drift of 1.80%. This indicated that the wall had a desirable ability to self-center after a seismic event. In general, the response of controlled rocking walls is dominated by rocking deformations as shown in Figure 1, while flexural and shear deformations are minimal [2, 3]. Because of the desirable self-centering response, several researchers have conducted further investigations in an effort to enhance the seismic performance of such systems [4, 5], including tests where masonry walls were used instead of their concrete counterparts [6].

The first study of unbonded post-tensioned controlled rocking masonry walls (PT-CRMWs) was conducted by Laursen et al. [6], where six fully-grouted walls, one partially-grouted wall and one ungrouted wall were tested. More recently, Hassanli et al. [7] tested four fully-grouted PT-CRMWs with different initial prestressing to yielding stress ratios and different PT bar distributions. Overall, the experimental results demonstrated that the behaviour of fully-grouted PT-CRMWs was similar to that of precast concrete walls pertaining to the self-centering ability and the localization of damage. However, there is still a need to quantify the seismic performance factors (e.g. R) for PT-CRMWs. In this respect, a methodology has been proposed in FEMA P695 [8] to evaluate the seismic performance factors assigned to a seismic force resisting system. The methodology considers the uncertainties associated with the ground motion, design, modelling, and test data in a probabilistic collapse risk assessment. The acceptance criteria of this methodology are defined based on achieving an acceptable collapse margin ratio (CMR) between the median collapse spectral intensity of a suite of ground motions, and the spectral intensity of the maximum considered earthquake (MCE).

In this paper, a simplified multi-spring numerical model is built using OpenSees [9] and used to assess the seismic collapse risk of PT-CRMWs following the FEMA P695 methodology [8]. For this study, the seismic response modification factor (R) used for designing the PT-CRMWs is taken as 5, similar to that currently assigned for special reinforced masonry walls (SRMWs) by ASCE/SEI 7-16 [10], to facilitate a direct comparison between both wall systems. The floor used is a precast hollow core with 2-inch topping that is expected to allow rotation during wall uplifting.

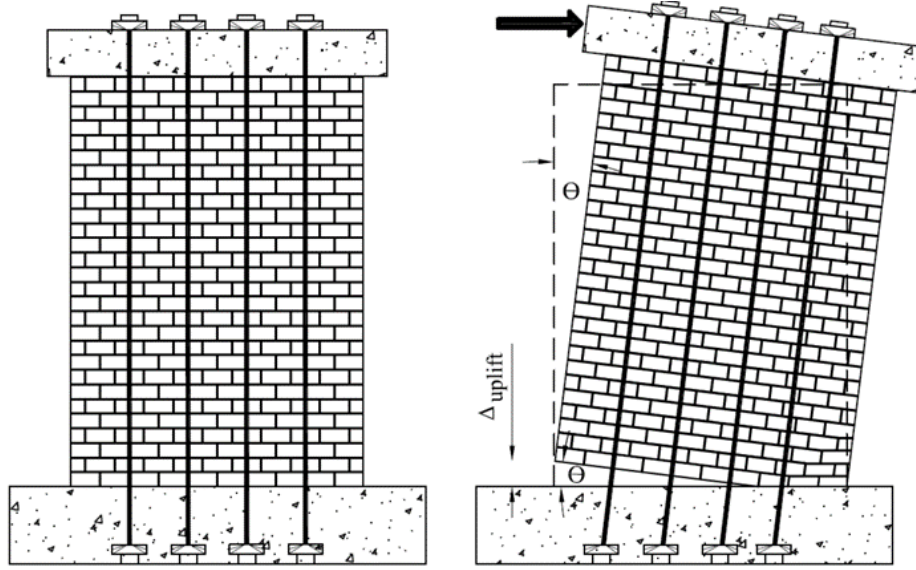


Figure 1. Unbonded post-tensioned controlled rocking masonry wall rocking mechanism

DESIGN OF PT-CRMWS

The current study is based on three of the 20 archetypes with fully-grouted SRMWs that NIST (GCR 10-917-8) [11] reported in its study to investigate the FEMA P695 [8] methodology. These three walls were redesigned as PT-CRMWs as described below. Full details about the wall dimensions and configurations are provided in Appendix A of the NIST (GCR 10-917-8) study [11].

The three archetypes (Walls PT-CRMW1, PT-CRMW2 and PT-CRMW3) were designed using the same seismic performance factors assigned for SRMWs (i.e. $R=5$) to facilitate a direct comparison. The PT-CRMWs were designed and detailed in accordance with the requirements of the TMS 402/602-16 [12]. For unbonded PT concrete walls, ACI 318-14 [13] requires that PT tendons remain elastic to ensure the self-centering ability of the walls under seismic loading demands. In a similar way, all PT tendons were designed to have lower stress demands than the corresponding yield strength, f_{py} , at the ultimate stage. However, the stress determination of the unbonded PT tendon at the ultimate stage, f_{ps} , is challenging because its elongation depends on the local base deformation of the wall at the corresponding base rotation. To address this, TMS 402/602-16 provided Eq. (1) to estimate f_{ps} , while previous research studies from Wight and Ingham [14] and Hassanli et al. [15] have provided Eq. (2) and (3), respectively, to estimate the same parameter.

$$f_{ps} = f_{se} + 0.03 \left(\frac{E_{ps}}{L_{un}} \right) \left(d - 1.56 \frac{A_{ps} f_{ps} + P}{f_m L_w} \right) \leq f_{py} \quad (1)$$

$$f_{ps} = f_{se} + \left(\frac{(h_w/L_w) \varepsilon_{mu}}{30 (f_m/f_m')} \right) \left(\frac{E_{ps}}{L_{un}} \right) \left(d - \frac{f_m L_w}{\alpha \beta f_m'} \right) \leq f_{py} \quad (2)$$

$$f_{ps} = f_{se} + \left(\frac{L_p (\varepsilon_{mu} - \varepsilon_0)}{c} \right) \left(\frac{E_{ps}}{L_{un}} \right) (d - c) \leq f_{py} \quad (3)$$

where f_{se} is the effective stress in the PT tendon after immediate losses, E_{ps} is the PT tendon modulus of elasticity, L_{un} is the tendon unbonded length, d is the distance from the tendon location to the outermost compression fiber, A_{ps} is the PT tendon cross-section area, P is the gravity load including the wall self-weight, L_w is the wall length, h_w is the wall height, f_m is axial compressive stress on the wall, L_p is the equivalent plastic hinge length, ε_{mu} is the masonry crushing strain, ε_0 is the masonry

strain corresponding to the decompression stage (defined as the stage when the wall is about to uplift), α and β are the equivalent stress block parameters [i.e. taken as 0.8 as per the TMS 402/602-16], and c is the length of compression zone. In the current study, Eq. (3) was used to calculate the stress in the unbonded PT tendon, and in the subsequent calculation of the flexural nominal strength (M_n), because Hassanli et al. [15] demonstrated that Eq. (3) provided the most accurate results.

For the one- and two-storey archetypes (PT-CRMW1 and PT-CRMW2), unbonded PT strands were used, while unbonded PT bars were used for the 4-story archetype (PT-CRMW3). This is because the high yielding strain capacity of PT strands compared to that of PT bars was needed to accommodate the high strain demands associated with the short unbonded length L_{un} of the one- and two-storey archetypes. In all cases, L_{un} is taken as the wall height plus 500 mm to account for the anchorage distance and embedded length in the foundation. The prestress ratio (i.e. the ratio of the initial PT stress to the yield strength), η , was set to be 0.5 for PT bars, where the yield strength is taken as 850 MPa [16]. Conversely, for PT strands, η , is taken as 0.25 to avoid premature yielding, with f_{py} taken as 1680 MPa [16]. Table 1 summarizes the masonry compressive strength, wall dimensions, and reinforcement details at the first storey for all three archetypes.

Table 1. Dimensions and Reinforcement Details of PT-CRMWs

Archetype ID	f'_m (MPa)	H_w (mm)	L_w (mm)	t_w (mm)	PT Area (mm ²)	d_{PT} (mm)	ρ_v (%)	Horizontal reinforcement (mm)	ρ_h (%)
PT-CRMW1	10.4	3657	7315	203	5x140	15.2	0.047	#5@1,220	0.085
PT-CRMW2	17.3	6096	9754	203	4x140	15.2	0.028	#6@800	0.180
PT-CRMW3	20.7	12192	9754	203	2x551	26.0	0.055	#5@800	0.127

The compressive strength of the unconfined masonry, f'_m , varied from one archetype to another in the NIST (GCR 10-917-8) study [11], as listed in Table 1. As such, the same values were used to design and model each corresponding PT-CRMW archetype in the current study. Figure 2 shows that one duct at the wall mid-cell was used for PT-CRMW1 and PT-CRMW2, while two ducts, spaced at 610 mm, were used inside wall PT-CRMW3.

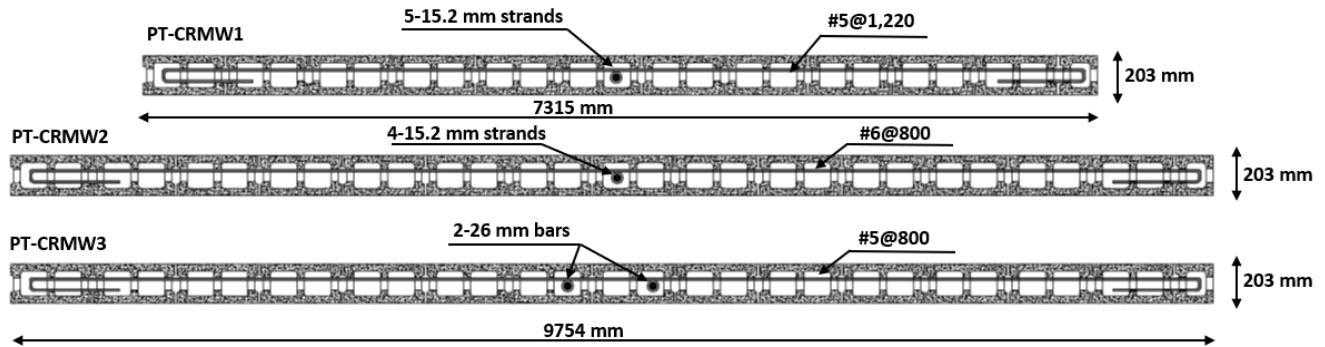


Figure 2. Walls cross-section details

Table 2 presents the seismic design parameters of the PT-CRMWs, including the response modification factor, R ; the prestressing ratio, η ; the gravity load intensity; the seismic design category SDC); the seismic base shear coefficient, V/W (where V is the base shear and W is the seismic weight); the MCE spectral acceleration, S_{MT} ; the code-defined estimate of the fundamental period, T ; and the fundamental period of the numerical model, T_1 . In the current study, T was calculated as $C_u T_a$ but limited to the lower bound value of 0.25s as recommended in FEMA P695 [8], where T_a is the approximate fundamental period and C_u is the coefficient for the upper limit on the calculated period. The calculated values of T_1 were based on the modulus of elasticity of masonry, which was taken as $900f'_m$ [12], and the effective moment of inertia, I_{eff} , which was taken as 50% of the uncracked moment of inertia of each masonry shear wall, I_g .

Table 2. PT-CRMWs Archetypes Design Parameters

Archetypes ID	Archetype design parameters								
	Number of stories	R	η	Gravity loads (% f'_m)	SDC	V/W	S_{MT} (g)	T (s)	T_1 (s)
PT-CRMW1	1	5	0.25	0.82	D _{max}	0.20	1.50	0.25	0.18
PT-CRMW2	2	5	0.25	2.50	D _{max}	0.20	1.50	0.26	0.14
PT-CRMW3	4	5	0.50	4.20	D _{max}	0.20	1.50	0.45	0.22

NUMERICAL MODELLING OF PT-CRMWS

The three PT-CRMWs were modelled using OpenSees, where Figure 3 shows a schematic diagram of the model including the distribution of elements for the four-story wall (PT-CRMW3). The model contains four primary elements: 1) an elastic Timoshenko beam-column element to model the wall considering its shear deformations; 2) a bed of zero-length spring elements to represent the wall-foundation rocking interface; 3) truss elements to simulate the PT tendons; and 4) an elastic beam-column element for the leaning column, to represent the gravity system associated with the wall and subsequently capture the P-Delta effects. The material model used for the zero-length springs was Conc01 in OpenSees, while a Giuffre-Menegotto-Pinto model (Steel02 in OpenSees) was adopted for the PT tendons, with an initial stress assigned to represent the initial prestressing force, T_o , applied to the unbonded tendons. Full details about the model validation can be found in Yassin et al. [17].

Initial stiffness- and mass-proportional Rayleigh damping was used in the current study following the same approach as NIST [11], but only the linear elastic frame elements (i.e. neither the PT nor the spring elements) were assigned stiffness-proportional damping. The Rayleigh damping parameters were calculated for the PT-CRMW3 archetype using a damping ratio of 5% at the first and third modes (ω_1 and ω_3), while for the one- and two-storey walls (PT-CRMW1 and PT-CRMW2, respectively), ω_1 and $5.0 \omega_1$ were used instead. For each wall, the seismic mass of each floor was assigned in both the horizontal and the vertical degrees of freedom, so as to include any effect of wall impact with the foundation.

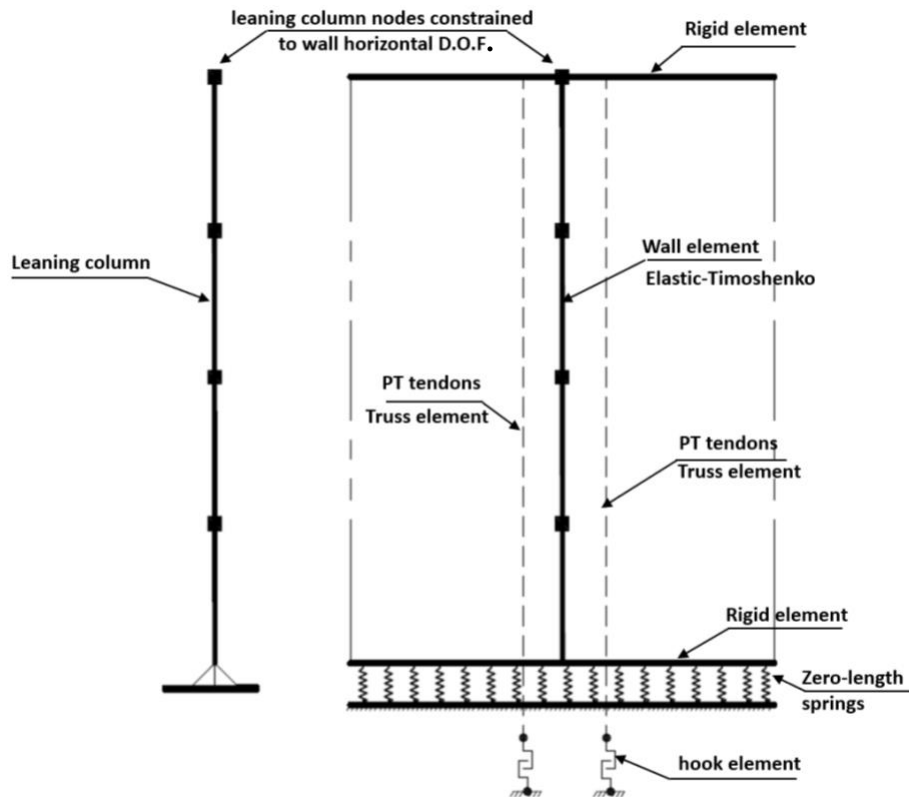


Figure 3. Schematic of numerical model for PT-CRMW3

NON-LINEAR DYNAMIC ANALYSIS AND COLLAPSE CRITERIA

A nonlinear dynamic analysis was performed for each archetype using the set of 44 far-field ground motion records provided as part of the FEMA P695 methodology [8]. As recommended there, the ground motion records were normalized by their respective peak ground velocities to exclude any inherent variability and the records were then scaled until the median value of the records match the MCE elastic design spectrum at the fundamental code-based period, T . Figure 4 compares the response spectra of the 44 normalized ground motions and their median spectrum to the MCE design spectrum for SDC D_{max} .

Dynamic analyses were conducted to calculate the probability of collapse of the three archetypes at different earthquake intensities. The results are presented using the Multiple Stripe Analysis (MSA) method, where the fragility parameters are calculated from the observed data by counting the number of collapses occurring for each scaled intensity measure [18]. In the

current study, all the ground motion records were scaled from 50% to 400% of the MCE at 50% increments, leading to a total of 8 stripes.

For the analyses in this study, collapse was defined following the NIST study [11] as the point when the wall reaches any of the following three conditions: 1) when 30% of the wall length reaches the crushing strain; 2) when a PT tendon reaches the fracture strain, taken as 0.02, which is one-third of the strain corresponding to ultimate strength to account for both low-cycle fatigue and anchorage stress concentration; or 3) when the wall reaches its shear capacity according to TMS 402/602-16 [12].

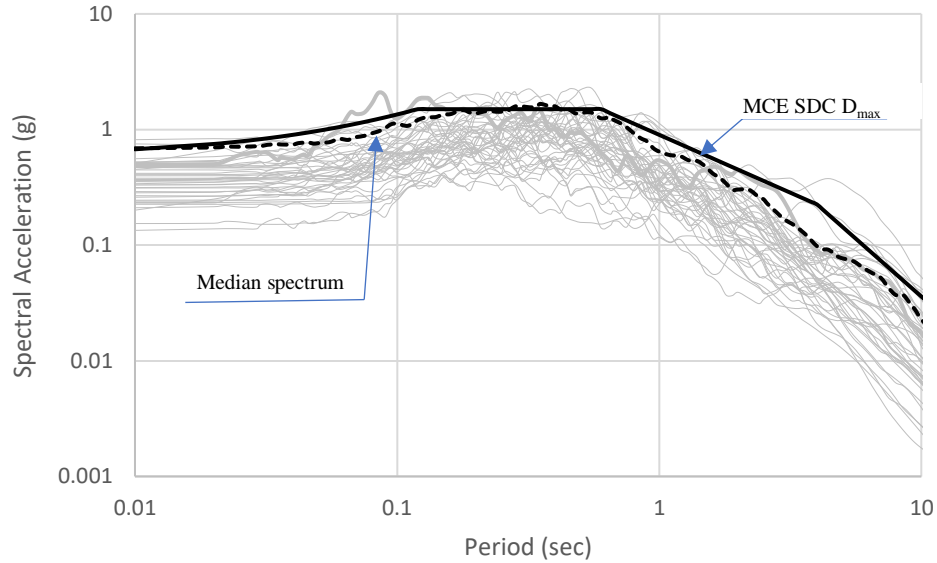


Figure 4. Response spectra of the 44-record set, their scaled median spectrum and MCE spectrum for SDC D_{max}

Collapse risk evaluation

For each archetype, the spectral acceleration of the MCE, S_{MT} , corresponding to the fundamental code-based period of the archetype, T , was determined. In addition, for each archetype, the median collapse spectral intensity, S_{CT} , defined as the spectral acceleration at which 50% of the records cause the structure to collapse, was determined through the MSA results. According to the FEMA P695 methodology [8], the collapse margin ratio (CMR) is calculated as presented in Eq. (4).

$$CMR = \frac{S_{CT}}{S_{MT}} \quad (4)$$

Table 3 summarizes the CMR values calculated from Eq. (4) for all PT-CRMWs archetypes considered in the current study. In addition, the CMR values that were reported in the NIST [11] study for SRMWs are shown also in Table 3 for comparison.

Table 3. Dynamic analysis results

Archetype ID	dynamic analysis results		
	S_{MT} (g)	S_{CT} (g)	CMR
PT-CRMW1	1.50	1.78	1.19 (0.52) ^a
PT-CRMW2	1.50	3.02	2.01 (1.14) ^a
PT-CRMW3	1.50	3.74	2.49 (1.55) ^a

^a Values for the corresponding Special RM walls reported by NIST [11] study

In the FEMA P695 methodology [8], the assessment criterion is achieved through the adjusted collapse margin ratio (ACMR). The ACMR is computed as the product of the spectral shape factor (SSF) and the CMR obtained from the MSA results, as presented in Eq. (5).

$$ACMR = SSF \times CMR \quad (5)$$

The SSF depends on the period-based ductility, μ_T , and the fundamental code-based period, T . The calculated values of the ACMR are then compared with acceptable values, which are given in FEMA P695 [8] in terms of the total system uncertainty, β_{TOT} , calculated from Eq. (6).

$$\beta_{TOT} = \sqrt{\beta_{RTR}^2 + \beta_{DR}^2 + \beta_{TD}^2 + \beta_{MDL}^2} \quad (6)$$

where β_{RTR} is the record-to-record uncertainty that arises from variations in frequency content and dynamic characteristics of the different ground motions along with variability in the hazard characterization as reflected in the ground motion records. FEMA P695 [8] assigns a value of 0.4 for β_{RTR} for systems with a μ_T greater than or equal to 3.0, which applies to the current study as presented in Table 4. In addition, β_{DR} accounts for the robustness and accuracy of the design requirements, β_{TD} describes the robustness and quality of the test data that are used to define the system, β_{MDL} represents model uncertainty. The three uncertainties β_{DR} , β_{TD} , and β_{MDL} were all assigned a rating of Good, with a corresponding value of 0.2, yielding a total system uncertainty β_{TOT} of 0.529. The FEMA P695 [8] methodology evaluates the seismic collapse risk using two acceptable ACMR values, which are defined based on total uncertainty associated with the system (β_{TOT}). The first is $ACMR_{20\%}$, which is defined as 1.56 for β_{TOT} of 0.529, to ensure a probability of collapse less than 20% for each individual archetype. The second value is the acceptable $ACMR_{10\%}$, which is 1.96 in this case to ensure an average probability of collapse less than 10% across the performance group. Both acceptable values must be satisfied to pass the performance evaluation as per the methodology. The results of the performance evaluation are shown in Table 4, where the values of ACMR for all archetypes are compared with the acceptable ACMR for both systems (i.e. PT-CRMWs and SRMWs). As can be seen from Table 4, the ACMR values calculated for PT-CRMWs exceed the acceptable ACMR values, indicating that using a response modification factor of $R = 5$ provided an acceptable collapse safety margin. Conversely, the SRMWs did not pass the methodology, because applying $R = 5$ resulted in a probability of collapse higher than 20% for one- and two-storey walls. This confirms the enhanced performance of PT-CRMWs relative to conventional fixed base SRMWs, when both wall systems are designed to have a similar strength.

Table 4. Collapse risk assessment

Archetype ID	Computed overstrength and collapse margin parameters				Evaluation check	
	CMR	μ_T	SSF	ACMR	Acceptable ACMR	Pass/Fail
PT-CRMW1	1.19 (0.52) ^a	25.71(5.20) ^a	1.33	1.58 (0.66) ^a	1.56	Pass (Fail) ^a
PT-CRMW2	2.01 (1.14) ^a	35.80(8.10) ^a	1.33	2.67 (1.52) ^a	1.56	Pass (Fail) ^a
PT-CRMW3	2.49 (1.55) ^a	18.48(11.80) ^a	1.33	3.31 (2.06) ^a	1.56	Pass (Pass) ^a
Mean of PG				2.52 (1.41) ^a	1.96	Pass (Fail) ^a

^a Values for the corresponding Special RM walls reported by NIST [11] study

Influence of confining the masonry

To investigate the influence of confinement on the collapse margin ratio of PT-CRMWs, the response was re-evaluated assuming that the masonry behaviour was enhanced by adding confining plates [19] at the bed joints between blocks. These plates were added only within the equivalent plastic hinge length, L_p , calculated using the expression provided by Hassanli et al. [20]. In this study, the ratio between the confined and unconfined crushing strains, λ , was set as 2.5 when determining the dimensions of the confining plates. Based on the collapse data from the MSA, a collapse fragility curve was defined as a cumulative distribution function (CDF) that relates the ground motion scaling intensity to the probability of collapse. Figure 5 compares the collapse fragility curves of the three walls for both confined and unconfined walls to demonstrate the influence of the confining plates.

As can be seen in Figure 5, S_{CT} is increased by 19% and 24% for walls PT-CRMW1 and PT-CRMW3, respectively, while wall PT-CRMW2 does not show an enhancement (fragility curves coincide). This is because wall PT-CRMW2 was governed by PT fracture, which can be enhanced by increasing the unbonded length of PT but not by confining the masonry, whereas walls PT-CRMW1 and PT-CRMW3 were governed by masonry crushing and shear failure.

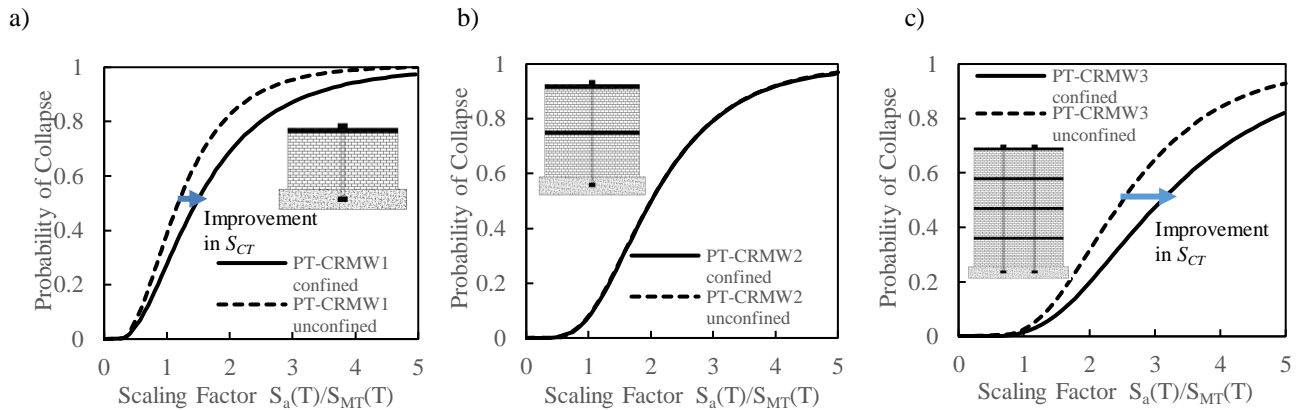


Figure 5. Collapse fragility results for a) PT-CRMW1, b) PT-CRMW2 and c) PT-CRMW3

CONCLUSIONS

This study evaluated the collapse risk of unbonded post-tensioned controlled rocking masonry walls (PT-CRMWs) under the maximum considered earthquake (MCE) when the seismic performance factors that are currently assigned to SRMWs were adopted for design. In this respect, three PT-CRMWs archetypes, each without and with confinement, were evaluated using the FEMA P695 methodology through a multi-spring model developed using OpenSees.

Whereas a previous NIST study [11] reported that low-rise SRMWs did not pass the FEMA P695 methodology, the results for similar PT-CRMWs considered in this study demonstrated that using an R factor of 5 meets the acceptance criteria of the methodology. This indicates that the R factor currently assigned for PT masonry walls (i.e. $R = 1.5$) is conservative for low-rise walls, either without or with confining plates. Finally, the results showed that the use of confinement plates within the wall bed joints clearly enhanced the median collapse spectral intensity, and subsequently increased the collapse margin of safety under the MCE.

Further research studies are still needed to include additional archetypes with different gravity load levels and numbers of storeys. These studies are expected to facilitate the adoption of unique seismic modification factors for PT-CRMWs within the next editions of relevant building codes and design standards.

ACKNOWLEDGMENTS

The financial support for this project was provided through the Canadian Concrete Masonry Producers Association (CCMPA), the Canada Masonry Design Centre (CMDCC), the Natural Sciences and Engineering Research Council (NSERC) and the Ontario Centres of Excellence (OCE).

REFERENCES

- [1] Priestley, M. J. N., Sritharan, S., Conley, J. R., and Pampanin, S. (1999) "Preliminary results and conclusions from the PRESSS five-story precast concrete test building" *PCI Journal*, 44(6), 42-67.
- [2] Nakaki, S. D., Stanton, J. F., and Sritharan, S. (1999) "An overview of the PRESSS five-story precast concrete test building" *PCI Journal*, 44(2), 26-39.
- [3] Kalliontzis, D., and Schultz, A. E. (2017) "Improved estimation of the reverse-cyclic behavior of fully-grouted masonry shear walls with unbonded post-tensioning" *Eng. Struct.*, 145, 83-96.
- [4] Holden, T., Restrepo, J., Mander, J. B. (2003) "Seismic performance of precast reinforced and prestressed concrete walls". *Journal of Structural Engineering*, 129(3), 286-296.

- [5] Pérez, F. J., Pessiki, S., and Sause, R. (2004) “Experimental and analytical lateral load response of unbonded post-tensioned precast concrete walls” *ATLSS Report* no. 04-11, Department of Civil Engineering, Lehigh University, 2004.
- [6] Laursen, P. T. and Ingham, J. M. (2004) “Structural testing of large-scale posttensioned concrete masonry walls”. *Journal of Structural Engineering*, 130(10), 1497-505.
- [7] Hassanli, R., ElGawady, M., and Mills, J. (2016) “Experimental investigation of in-plane cyclic response of unbonded-posttensioned masonry walls” *Journal of Structural Engineering*, 142(5), 04015171-1-15.
- [8] FEMA (Federal Emergency Management Agency). (2009). “Quantification of building seismic performance factors.” *FEMA P695*, Washington, DC.
- [9] McKenna, F., Fenves, G. L., and Scott, M. H. (2000). “*Open system for earthquake engineering simulation.*” University of California, Berkeley, CA.
- [10] ASCE/SEI (Structural Engineering Institute). (2016). “Minimum design loads for buildings and other structures.” *ASCE/SEI 7-16*, Reston, VA.
- [11] NIST (National Institute of Standards and Technology). (2010). “Evaluation of the FEMA P695 methodology for quantification of building seismic performance factors.” *NIST GCR 10-917-8*, Gaithersburg, MD.
- [12] TMS (The Masonry Society). (2016). “Building Code Requirements and Specification for Masonry Structures” *TMS 402/602-16*, Longmont, CO.
- [13] ACI (American Concrete Institute). (2014). “Building code requirements for structural concrete.” *ACI 318-14*, Farmington Hills, MI.
- [14] Wight, G. D., and Ingham, J. M. (2008) “Tendon Stress in Unbonded Posttensioned Masonry Walls at Nominal In-Plane Strength” *Journal of Structural Engineering*, 134(6), 938-946.
- [15] Hassanli, R., ElGawady, M., and Mills, J. (2017) “Simplified approach to predict the flexural strength of self-centering masonry walls” *Eng. Struct.*, 142, 255–271.
- [16] DSI (DYWIDAG Systems International). (2015) *DYWIDAG Post-Tensioning System using Bars*.
- [17] Yassin, A., Ezzeldin, M., and Wiebe, L. (2019) “Numerical modelling of controlled rocking post-tensioned fully-grouted masonry shear walls with and without energy dissipation” *13th North American Masonry Conference*, Salt Lake City. (under review)
- [18] Baker J. (2015) “Efficient analytical fragility function fitting using dynamic structural analysis” *Earthquake Spectra*, 31(1), 579–599
- [19] Priestley, M. J. N. and Elder, D. M. (1983) “Stress-strain curves for unconfined and confined concrete masonry” *ACI Journal*, 80(19), 192-201.
- [20] Hassanli, R., ElGawady, M., and Mills, J. (2015) “Plastic hinge length of unbonded post-tensioned masonry walls” *12th North American Masonry Conference*, Denver.